

Biomechanism Profile of Intervertebral Disc's (IVD): Strategies to Successful Tissue Engineering for Spinal Healing by Reinforced Composite Structure

Kunal Singha^{1*} and Mrinal Singha^{2*}

¹Department of Textile Technology, Panipat Institute of Engineering & Technology, Hararyana, India

²Department of Pharmaceutical Chemistry, CU Shah College of Pharmacy & Research, Gujarat, India

Abstract

Complex multi-lamellar biocomposite structure of Intervertebral Disc (IVD) imparts flexibility between adjacent vertebrae, as well as allows transmission of loads from one vertebra to the next along the spine. The disc has a 15- 25 concentric layered laminate structure; each layer is reinforced by collagen fibers which are aligned at approximately 30 degree angle in successive layers with respect to the transverse plane of the disc. This fibrous organization is critical to the proper biomechanical functioning of the disc, such as to convert compressive force to lateral force, to withstand extrinsic tensile stresses (circumferential, longitudinal and torsion). As a result spine becomes flexible to bend and twist. With the regular aging the disc gets dried up lost its flexibility and biomechanical elasticity. That's why we need tissue engineering of that degenerated tissue to make a proper ailment of that body part by the help of some textile fibers like silk- hydrogel, CMC, PVA- collagen, PGA – chitosan composites. The synthetic polymer has shown great promise for easiness of production, variability in properties and biodegradability and biocompatibility and non-immunogenic response inside the human spinal body for the novel cause of removal and restoration of degenerated human intervertebral disc.

Keywords: IVD disc; Nucleus pulposus; Biomechanical functioning; Tissue engineering; Silk- hydrogel; CMC; PVA- Collagen; PGA - Chitosan composites

Abbreviations: IVD: Intervertebral Disc; AF: Annulus Fibrosus; NP: Nucleus Pulposus; EP: End Plate; CMC: Carboxymethyl Cellulose; PVA: Polyvinyl Alcohol Fiber; PGA: Polyglycolic Alcohol Fiber; TE: Tissue Engineering; MMPs: Matrix Metalloproteinase's; ADAMTS: A Disintegrin and Metalloproteinase with Thrombospondin Motifs; TIMP-1: Tissue Inhibitor of Metalloprotein; PCL: Polycaprolactum Fiber; ECM: Extra-cellular Matrix

Introduction

Lower Back Pain is a common clinical complaint in these present days. In fact most of these symptoms are rises from the biomechanical sources, and the Intervertebral Disc (IVD) is the main culprit in that case. IVD rests in the spinal cavity with the help of huge body pressure, compression force due our body weight (BW) and normal body movement [1,2] and given their close proximity to the spinal cord and other peripheral nerves [3,4], it is no surprise that complications with the IVDs can lead to serious neurological effects and become detrimental to multiple areas of the body and the complex loading behaviour [5] of the cervical discs and their frequent involvement in pain and pathology, it is important to understand their mechanical properties. In human body we can three types of cartilage tissue (network of highly densed connective tissue) like (i) annulus fibrous tissue (AF tissue) – present in synovial bone joint [6] (ii) elastic cartilage – present in outer ear, larynx and epiglottis [7] (iii) fibro cartilage – present in IVD, meniscus, temporomandibular joint [8]. So IVD is basically a fibrocartilage type of body tissue, when the jelly like NP matrix prolapsed it forced out to rupture outward and thus creating a pressure on its surroundings nerve tissue or column and these may leads to symptoms of sciatica [9,10,11]. IVD or simply so called disc is consist of mainly three parts (i) NP (Nucleus Pulposus) the inner jellylike substance at the centre part of the disc which primarily contribute to the torsional or twisting movement of the body, (ii) AF (Anulus Fibrosus)- the outer soft

biological tissue part relatively much stronger than NP that is the central part relatively easily deformable and that is the peripheral part [12,13], mainly distribute the stress on spine and degeneration of these part is mainly responsible for LBP (lower back pain). AF governs all the mechanical properties like viscoelasticity [14], hyperporoelastic mechanical profile [15], aggregate or elastic modulus, permeability or disc tissue porosity, anisotrochical or heterogenetical biomechanical characterization. AF part also governs four main biomechanical spinal disc manifestations like: stress-strain rate trend, hysteresis, creep [16] and stress relaxation from the mechanical deformation. (iii) EP (End Plate) is the peripheral subcutaneous bony part which surrounds the IVD or disc ring for protection helps in disc recovery. EP is generally the subchondral bone layer and maintains the contact between IVD and spinal cord (SC). It has no relation with LBP. The fluids flow inside the end plate play a main role for the recovery of the disc in vivo but in case of in vitro the role has limited (Figure 1). With ageing normally the AF layers gets dehydrated due to loss in hydration [17], so the disc bulging and finally gives enormous pressure to its surrounding symptomatic spinal nerves (C3-C4: cervical nerve roots) by the disc protrusion- which may cause chronic back pain [18,19,20]. So the main concern about successful disc repairmen

***Corresponding authors:** Kunal Singha, Assistant professor, Department of Textile Technology, Panipat Institute of Engineering & Technology, Hararyana, India, Tel: +091-9355928123; E-mail: kunalsingha28@gmail.com

Mrinal Singha, Assistant Professor, Department of Pharmaceutical Chemistry, CU Shah College of Pharmacy & Research, Gujarat, India, E-mail: mrinalsingha@gmail.com

Received January 11, 2012; **Accepted** June 15, 2012; **Published** June 18, 2012

Citation: Singha K, Singha M (2012) Biomechanism Profile of Intervertebral Disc's (IVD): Strategies to Successful Tissue Engineering for Spinal Healing by Reinforced Composite Structure. J Tissue Sci Eng 3:118. doi:10.4172/2157-7552.1000118

Copyright: © 2012 Singha K, et al. This is an open-access article distributed under the terms of the Creative Commons Attribution License, which permits unrestricted use, distribution, and reproduction in any medium, provided the original author and source are credited.

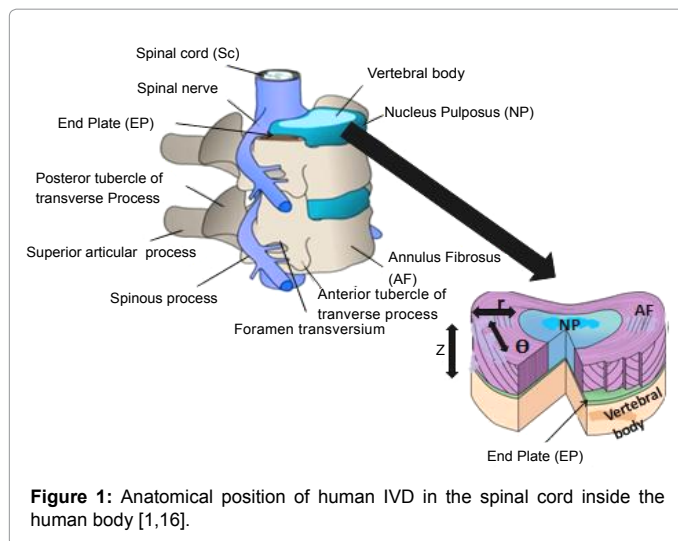


Figure 1: Anatomical position of human IVD in the spinal cord inside the human body [1,16].

is to synthesised and simulate the biomechanical and kinematics properties [21,22] of that AF tissue layers. For that purpose goat IVD is used to carry out the biomechanical experiments to study the native disc biomechanics. Goat IVD is used because it has almost similar kinematics and dynamic profile under loading or stress like in case of human IVD [23]. Besides that the silk based novel scaffold (fibre-hydrogel ECM (extracellular matrix) composite) [24] has been also carried out to various mechanical testing to check out the proximity of their mechanical properties to the native goat AF tissue construction. AF is approximately a ring (some of the ring of complete and continuous and some of them are incomplete and discontinuous) like angle-ply structure where the collagen II fibers [25,26] are specially oriented $+30^{\circ}$ / -30° in above and in below the transverse plane of the body spinal axis [27,28,29]. The AF structure is more complex than NP structure because it consist of circumferentially discontinuous and traversed by fibrous assembly that runs radially outwards from the spinal axis [30,31,32,33]. Due to special arrangement of the fiber in the AF layers these layer can take more load bearing capacity (like mainly compression, torsion, shear, tensile etc.) [34,35,36] by readily resolving the uploaded body force on it. Also the Poisson's ratio of NP is lower than the AF; so AF got higher degree of deformation [37,38] in it so the biomechanics of AF is our main concern than NP layers [39,40].

Scope rationale of this review

The review will address progress made in polymeric implants over the last decade, dealing primarily with spinal therapeutic devices and replacements. The review is mainly includes the followings;

- a. Biomechanics of the spinal intervertebral disc or cartilage
- b. Polymeric materials or scaffolous substrates which are being used for replacement of spinal lower back pain.

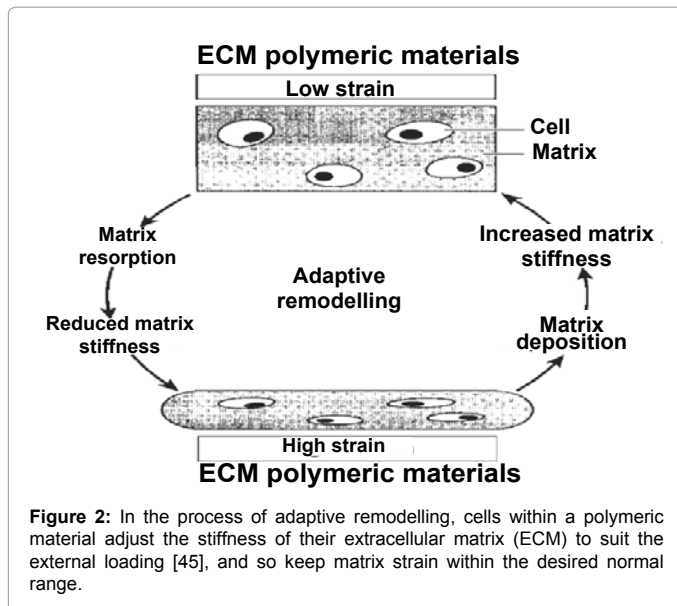
In today's world full of heavy work load the medical problems becomes stronger day by day in everyone's life. Lower back pain (LBP) is most common type of medical disease which cause near about 7 million people in UK in every year. LBP generally produced due to the malnutrition of the cartilage inside our spine. This small cartilage discs are called intervertebral disc (IVD) which mainly bears 90% of our body load with the incorporation of our spinal body axis. With aging the disc gets dehydrated and loss in its height therefore as the result it collapsed toward the cervical nerves and

produce severe back pain and sometime obesity also. The ways to remedies for that are taking regularly pain-killer tablets, anesthetic, fixing of unhealthy disc and fusion of the disc but in all this process the patient lose their natural flexibility and body movement due to the heavy weight of that non-biodegradable, non-biocompatible material. The current object of this review paper is to make use of Tissue Engineering (TE) with the help of making scaffold hydrogel by the help of some textile material like: silk, CMC, PVA, PGA, PCL-collagen composite material. This scaffold composite material can bear the same bio-mechanical properties with superb bio-compatibility and bio-degradability, also they are very light in weight and easy to replace inside the patient body. In this current paper we had also discuss about the different mechanical force can acts inside a disc matrix and the measurement techniques generally used those forces. The others alternatives options are also discuss which can be very handy in disc therapy besides the tissue engineering. The working principle involved for an ideal scaffold material has been also discussed which is very important for a successful disc replacement with the help of tissue engineering techniques.

Spinal therapy

The spinal therapeutic broadly cover both the herniation of interverbral disc and the damage of the articular ligaments. This review specially limited and focuses on the herniation or degeneration and procurement of the intervertebral disc. We specially consider the biomechanics of the disc as the disc profile and behavior is fully controlled by the disc biomechanology and elasticity (loss of elasticity) and flexibility. The tensile, compressional, torsional, hyperflexion [41] of neural arch and shear force behavior is very important to predict the disc anatomy and body-load bearing capacity. This is the first and primarily most important focus of our discussion. In general, spinal disc herniation gives the patients symptomatic nerve pain which is amenable to treatment with removal of the herniated part of the disc or with the disc angioplasty [42] which may vary from patient to patient and totally artificial. Other spinal disc therapeutic conditions such as fixing the screw after removal of the degenerated disc or a ceramic-cement fixation over the spinal cord [43,44], but these techniques fails due to the reason that the patient loss natural movement and flexibility of own's spinal cord and body weight seems get heavier. There is also a chilled feel due to the metallic screw uses inside the body during the change of the seasonal weather and the immune response and non-biocompatibility of this type of foreign substrate is become very detrimental for the patient in the future. For all of those above constraints, this all later techniques are fall these falls outside the scope of this review.

Polymeric biomaterials are generally derived from three sources: natural polymers, including those of plant and animal origin; totally synthetic sources; and synthesis based on materials of natural origin. The first two categories are self-explanatory; the third is of relatively recent vintage. It encompasses materials synthesized to mimic a naturally occurring polymer, but not necessarily identical to it. The most important materials in this category are the man-made protein structures, which resemble natural proteins but differ from them in some details of the primary structure. This third class of polymers promises innovative materials that have the potential to functionally replace diseased or unavailable cell components, such as the extracellular matrix, which plays a structural role in many organs and tissues by the super ability of controlling the matrix stiffness (Figure 2) by the shock absorption capacity with the macro, micro or nano level inside the living tissue [40,41]. Within each application, we will highlight the



advances made in the development of each type of polymer, and the benefits they confer. This is the second focus of our discussion.

Types of implantable polymers

Synthetic polymer have been wide used as the implantable materials due to the reasons include ease of production; control over the properties of the polymer during spinning and over of its end products; ready availability and versatility of manipulation. Conversely the polymer from natural resources likes collagen being variable on its properties from source to source; possibility of bacterial and viral contamination and chances of antigenicity is not being very popular implantable materials. If these organic materials are of animal origin, there are added complication of harvesting the polymer or protein and purifying it. For these reasons, synthetic polymers have dominated the spinal implantable therapeutic landscape. For examples, the alginate/chitosan electrospun, poly-methylmethacrylate hybrid fibers provides the non-immunogenic spinal disc implants, electrospun PCL, electrospun PGA and alginate hydrogel can give suitable lamellar products with higher compressive composite materials under the implantation inside the body. The photocross-linked CMC can be used for encapsulated nucleus pulposus implants cells. It may also achieve the higher mechanical stiffness by atelocollagen-silicone composite, ultra-high MW polyethylene constructs as in a form of honeycomb structure due to its higher capacity of shock-absorption and flexibility of its matrix for the micro-interlamellar movements and moderate range of intrinsic viscosity between the hydrogel layers. In the recent days natural polymer like silk with rapid availability, versatility and huge mechanical stiffness and modulus can be used for spinal disc implantable materials as in a form of hydrogel where the fibers are orientated in a concentric circles with an opposite fiber direction to replicate the native disc anatomy; which gives the ultimate mechanical stress-relaxation capacity and simulation with the original disc mechanology. All of these above mentioned manmade polymers can be synthesized under controllable conditions with a predictable and control properties from batch to batch with almost no likelihood of microbial infection or contamination. Antigenicity cannot be fully achievable but still these polymers provide great promise for implantable materials, due to mainly the easiness of production that mimic and simulate the body's own structural anatomical architecture in terms of function and metabolic immunity.

Outline of the review

The discussion will address these aspects in each application:

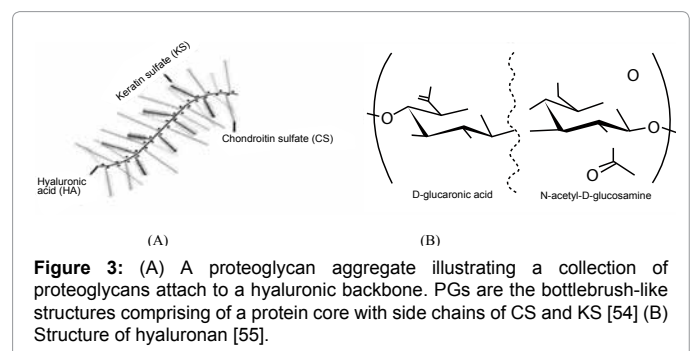
- The composition and SEM (scanning electron microscopy) image analysis of the intervertebral disc to get an idea about its structural parameter and components.
- The biomechanology of the disc with the details of various mechanical behavioral characteristics.
- Polymers that have been evaluated using in vitro methods
- Outcome of animal studies and (if available) human performance data for the benchmarking comparison of experimental and actual mechanical modulus of those polymeric implants.
- Commercial success.
- Others methods for disc healing except the tissue engineering implants methods.
- Future directions.

Compositions of IVD

The composition of IVD is shown in the Table 1. The 60-70% of the IVD is water [46,47]. The remainder is mainly PG (Proteoglycan) and collagens. PG is mainly consists of cell ground substances GAGs (Glycosaminoglycan) [48] which is primarily CS (Chondroitin sulfate) and KS (Keratan sulfate) [49,50] with the high molecular weight complex proteins, disaccharides [51]. This PG acts as the backbone of the HA (Hyaluronic acid) to make a macromolecules weight ~ 200 millions [52,53] (Figure 3). Approximately 30% dry weight of IVD is PG and there is always a variation in gradient of PG and water across the depth of the disc, in the upper subchondral bone layer the concentration of PG is less but water is high and inside the tissue concentration of the PG is high and water is less [51]. HA acts as the binding sites for CS and KS or makes the aggregate thus makes the big brush like macromolecules inside the IVD cells [46,53].

SEM analysis of native annulus fibrosus tissue

Goat's intervertebral discs (IVD) corresponding to L-1 to L-7 were dissected from the spinal column of 6-8 year old goat within 24 hours of slaughter from nearby slaughter house. Following dissection the discs were rinsed in PBS. Subsequently the disk tissues were finely cut with a sharp surgical blade ensuring uniform dimensions of (2 × 5 × 7) mm of annulus tissue sample (Figure 4). The specimens tested were cut to widths of 2.3 mm in accordance with American Society for Testing and Materials (ASTM) [56,57] standards maintaining a ratio



Components	AF	NP
Water	60-70 %, no change with age	90 % at birth 80 % at age 20 70 % at older age
Collagens (collagen I, collagen II, collagen X- collagen X is produced by the degenerated disc which has very poor mechanical properties)	Only collagen II, 50-60 % with (dry weight) Little change with age	Only collagen I, 15-20 % with (dry weight) Little change with age
PGs (Proteoglycans)	15-20 % with (dry weight) Little change with age	65% with (dry weight) Little change with age
Non- collagenous proteins and elastin	5-25% with (dry weight) Little change with age	20-45% with (dry weight) Little change with age
Extracellular enzymes, age pigments, cells	Minor remainder	Minor remainder

Table 1: Basic components of the IVD [46].

of 0.5 (ASTM 1990). After collection of those samples with proper dimension measurements are proceeds for the different mechanical testing characteristics techniques for IVD (for the mechanical testing was set at (1 mm/min).

The thickness of each AF layer increases towards the centre and the peripheral region the thickness is around ~ 100 µm where as near the centre the AF layer thickness is around ~ 150-175 µm [60,61] and the distance between two AF layers decrease towards centre (Figure 5).

SEM picture shows orientation of collagen fibers in AF layer +/- 30° in the alternative layer. This opposite angular position with a preferred fiber direction gives the opportunities for easy force resolutions under a small loading over the annulus tissue. Thus the disc can withstand it structural support and compatibility inside the spinal cord of human body and bears the body weight normally [62,63].

Mechanical Force Exerted on the IVD in the Spinal Cord

The healthy disc can be gets degenerated or unhealthy one due to the combine effects of mechanical loading precipitation, genetic inheritance, irregular loading history which may cause the generation of 'weak-link' in the anterior of the disc by breaking the 'shield-stress' layer inside the posterior lamellar domain or region of the disc. As a results, the anterior part of the disc is gets collapsed and form the degenerated or unhealthy (herniated disc) due the formation of 'wedge fracture' [64,65] in the anterior-posterior interface region of the disc. The percentage of the stress or body load bearing capacity is different for the healthy and unhealthy disc is being totally different due to the reason of the profile and surface contour or arial distribution of the collagen fiber, extracellular matrix over its structure [66]. Vertebral damage could cause back pain indirectly by generating high stress concentrations within the adjacent intervertebral discs (Figure 6) and subsequently could cause the annulus to collapse into the nucleus [67]. This mechanism is supported by a survey of adolescents, which confirmed that vertebral body damage is often followed by disc degeneration several years later [68].

Disc is tightly fitted in the spinal vertebral cavity under a huge compressive force [42]. So the main aspects to look for of these kind of tissue is study the compressive force or strength on it. The forces exerted on AF layer of the disc (Figure 7) are (i) compressive force (uniaxial (unconfined compression which is done normally), biaxial (confined compression- specially tested for soft biological tissue like AF, cartilage), triaxial compression) (ii) tensile force (uniaxial, biaxial, triaxial tension) (iii) shearing force (iv) torsional or twisting force and the (v) water hydrostatic force [44].

There may be three types of compression test can be done on AF tissue – uniaxial (only in Y- direction), bidirectional (both in

X-Y directions) and tridirectional (X-Y-Z directions) [44,45]. The unidirectional test is called as unconfined test and the bidirectional or tridirectional test is called confined test of AF tissue. In case of unconfined mechanical test we consider the amount of water and its hydraulic pressure contribution to the mechanical testing [70]. Normally under the impulsive compressive force or loads on the AF tissue experiences a large lateral displacement due to its high Poisson's ratio of about 0.5 [7]. This expansion is restrained by comparatively stiffer underlying subchondral bone which produced a higher shear stress (Figure 8) at the cartilage bone interface (cartilage- bone boundary)[71].

The Poisson's ratio (ν_s) of the native AF layer for goat IVD with by the using of following formula [56] by considering it as an uncompressible, poroviscoelastic material like the AF tissue by the following formula (1,2); $(E_s/H_a) = (1-\nu_s) / (1+\nu_s) (1-2\nu_s)$ (1)

Now by simplifying the above formula; we can get:

$$\Rightarrow 2\nu_s^2 + \nu_s a - a = 0 \text{ [where } a = 1 - (E_s/H_a)] \quad (2)$$

The positive root of these quadric equation will give us the Poisson's ratio of the material, Where H_a = aggregate modulus i.e. compressive modulus or strength (force), E_s = elastic modulus, ν_s = Poisson's ratio of the material respectively and E_s (MPa) = force at break of the material in compressive test / 1000 x % of elongation.

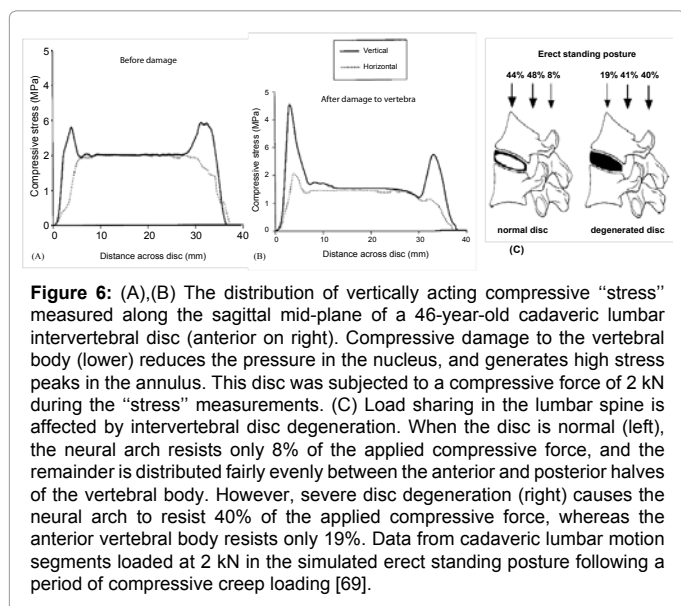
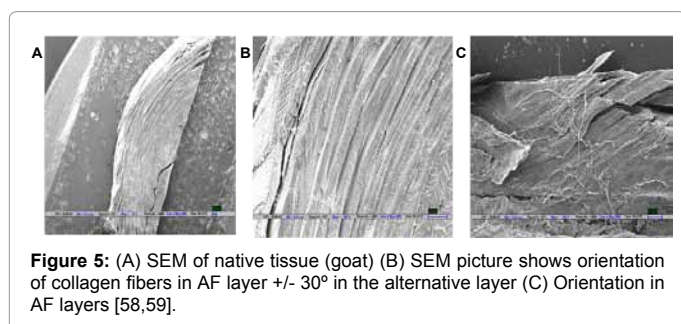
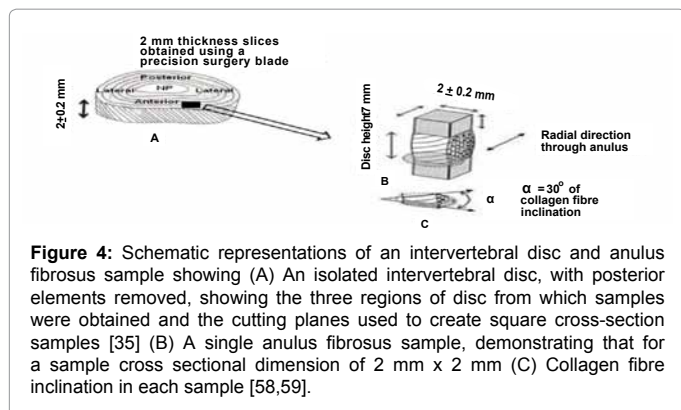
Compressive test

Compressive strength test has been carried out for large numbers of AF tissue with Hounsfield load cell force accuracy = 0.5% applied force [72,73]. Two types of - confined and unconfined compression test has been carried out and the compressive modulus is produced the higher value (Figure. 9(A)). The longitudinal and radial pressure on annulus tissue is proportionally increased with the magnitude of the compressive stress (load) Figure 9 (B), (C).

On loading upon in a typical displacement of annulus tissue in a confined test gives us a curve between displacement and time (Figure. 10(A)). Initially the deformation is rapid, as relatively large amounts of fluid (water) being going out from the annulus tissue. Then reaching at a constant value the displacement slows down after a certain time as the fluid flow slows to zero [74,75]. The material properties of annulus tissue are determined from this test. The typical compressive stress-strain behavior under uni-axial force and bi-axial force is shown is as in the Figure. 10(B),(C).

The total compression stress on the disc matrix is further carried out by different parts of the disc:

$$W_{total} = W_{matrix} + W_{fibre} + W_{shear.int.} + W_{normal.int.} \quad (1)$$



A stress-free reference configuration was ensured by enforcing $W_i(I) = 0$ for $i = \text{Matrix, Fibers, Shear Int, Normal Int}$. The sum of the structural terms, W , was required to be greater than zero: $W(C) \geq 0$. The Mooney–Rivlin model [65] for AF and NP tissue like anisotropic, nonlinear, hyper-oroelastic tissue material by the help of 9 parameter ($C_1, C_2, C_3, \dots, C_9$ and $a_0 = b_0 = d$) to determine and describe the FEM model [76,77] and to check-out the best-fit curve with our experimental curves [78]. All the analysis was done in the Lagrangian tissue strain dataset domain and the calculation of the contribution from the different component of the tissue comprises the Cauchy-Green deformation tensor, C , which was calculated from the Lagrangian strains using $C = 2E + I$ for use in finite- deformation stress-stretch

equations [79,80,81] best-fit curve with the experimental curves by the following formula (4,5,6,7,8);

$$I_1 = \text{tr } C, I_2 = 1/2 [(tr C)^2 - \text{tr } C^2] \quad (4)$$

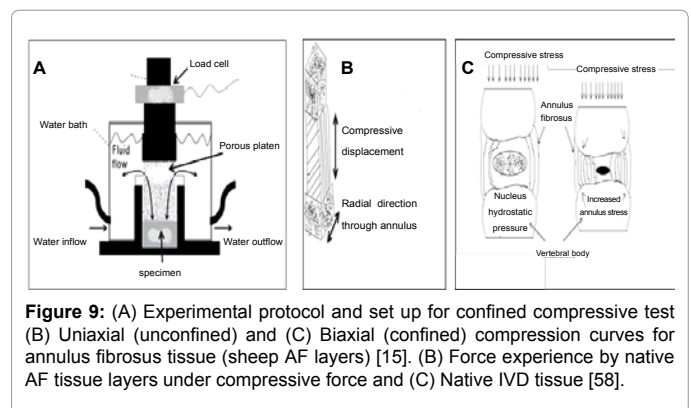
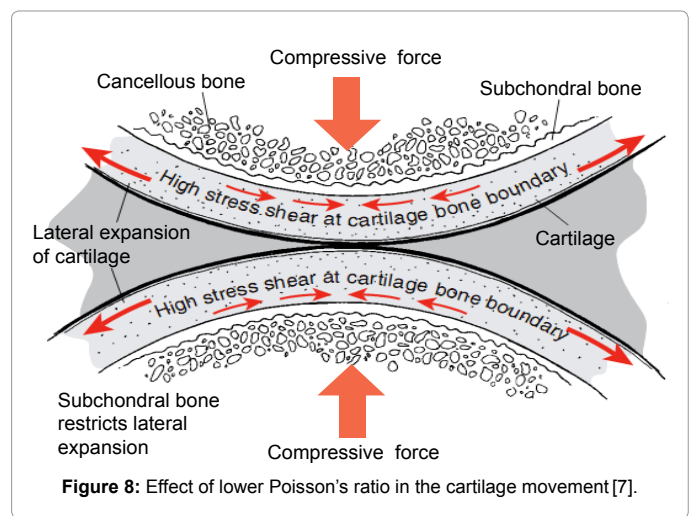
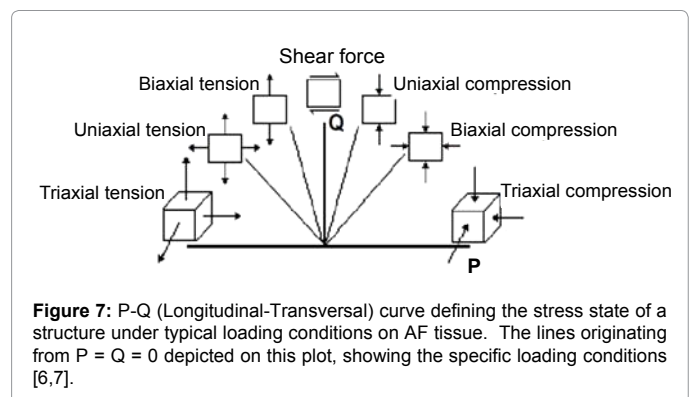
$$I_3 = \det. C, I_4 = a_0 \cdot C \cdot a_0 \quad (5)$$

$$I_5 = a_0 \cdot C^2 \cdot a_0, I_6 = b_0 \cdot C \cdot b_0 \quad (6)$$

$$I_7 = b_0 \cdot C \cdot b_0, I_8 = \cos(2\Phi) a_0 \cdot C \cdot b_0 \quad (7)$$

$$J = \det. F \quad (8)$$

Where; I_α = Lagrangian deformation [82,83] strain vectors working inside the AF tissue ($\alpha = 1, 2, 3, \dots, 8$), C = Right Cauchy-Green



deformation tensor [82,84], E = Stress tensor, 2Φ = Angle between the fiber populations inside the AF material matrix [85,86]. So from those above equation we get: $I_1 = I_3$ and $I_4 = I_5 = I_6 = I_7 = I_8$ as $a_0 = b_0 = d = 0$ (for soft biotissue like AF tissue) [87].

Simple shear test

Pure shear (no hydrostatic stress) [83] is a difficult stress state to achieve so simple shear test had been carried out by putting a simple shear stress. Then the equivalent pure shear state (stress and strain) was calculated with some mathematical formulae between pure shear strain energy density (U) and simple shear stress. The schematic experimental set-up has Figure 11 (A) and the stress-strain behavior of the AF Figure 11 (B) under a small shear force has been shown.

The value of shear force modulus [86] value is always less than compression modulus value because shear force is a biaxial phenomenon (X-Y plane velocity) unlike the compression or tensile which is an uniaxial velocity only. The value of the shear force modulus actually determines the interlaminar slippage between the fiber and the differential surface velocity between the fibers inside the annulus tissue matrix. The noted value of the shear modulus value of bovine annulus fibrosus is $21.3 \pm 2.3\%$ MPa [87] which is higher due to the hyperviscoelastic [88,89], porous and interlocked nature of the collagenous fibers and proteins inside the AF material's matrix. The value of shear force is poor in IVD because due to lack of sectional movements (sliding, gliding phenomenon inside the IVD matrix etc.) for highly porous and viscoelastic structure of AF tissue.

The interlamellar shear strain is due to the conjoint results of skewing and stretching or slipping of the ply oriented AF tissue material at its peripheral or circumferential areas. The collagen and elastic fibres located along the ply boundaries are radially oriented and the localised concentration of radially orientated collagen fibres [90] are divided in multiple plies in minutely distributed cross bridge architecture. The AF tissue is a perfect example of composite material where the

micro-failure does not normally occur in a single loading and instantly because this composite laminated structure can effectively resist crack propagation and requires multiple cracks and micro-failure to occur prior to final failure of the laminate [91], while more homogeneous structure needs a single crack to failure. Typically annulus tissue needs damage initiation by various modes like fibres pullout from the matrix, matrix deterioration by cracking, excess longitudinal tension and then damage accumulation by fibres buckling which leads to final failure of the tissue [92]. Failure chances due to cracking increases with aging as the numbers of degenerated circumferential plies of cartilage increases and thickness of each layer increases. For this reason the potential of interlaminar shear stress increases due to over delimitation probability of the relative weaker fibrous part of annulus tissue [93] and to know more better about the micro-mechanics of the annulus tissue Cartesian coordinate system had been already applied to a particular rectangular region of the specimen called region of interest by the various researchers. They had used particle image velocimetry (PIV) technique to quantify the shear factors but somehow were not able to determine the values of various shear factors [94]. Generally the polar co-ordinates (X, Y, Z, θ) are widely used to find out the amplitude of the average angle, angle of inter-annulus layer shear orientation during this whole study and analysed the micro-structural assumption in longitudinal and transverse direction inside the specimen by building up a lamination theory in axial, circumferential and radial mode [95]. This idea needs an assumption that $\pm\theta$ angular deformation is always held in consecutive plied layers in the AF tissue and only the boundary layer having the highest degree of free movement freedom with the appropriate co-ordinate shear mechanics [96]. The inter-shear force production is strictly dependant on the angle of dynamics created at the time of shear test and the length of the specimen tested, which is determined by the following formula (9,10);

$$\Theta^* = 2 \left| \tan^{-1} \left[\left(\frac{1}{\tan \Theta_0} + \tan \gamma \right)^{-1} - \Theta_0 \right] \right| \quad (9)$$

$$l^* = 2 \left[\left[\cos \Theta_0 + \sin \Theta_0 \tan(\gamma)^2 + \sin^2(\Theta_0)^2 \right]^{1/2} - 1 \right] \quad (10)$$

Where l^* = simple shear stretch, Θ^* = angle of rotation or shear angle, γ = strain amplitude ($\Delta L / L$ at sample initial length, $L = 7$ mm, ΔL = deformation) depending upon average angle of orientation of collagen bundle at $\Theta_0 = 30^\circ$.

Tensile test

Tensile test was done by loading for circumferential loading for axial loading. Each annulus tissue was loaded five times to a maximum strain of 55-60% and the specimens were permitted to relax for 5 minutes in between the load application. In all those above experiments sheep disc (AF tissue) has been used because sheep (goat) disc follows almost same kinematic and biochemical properties to human discs [97]. The time dependent response of the annulus tissue is very difficult to establish under in vitro environment due to lack of time-dependent transient equilibrium state, so we used the near linear region after the non-linear "toe-in" region [98,99] to estimate the Young's modulus where all the collagen bundle are straightened out [100] due to the tensile loading and stretching. Depending upon the stress-strain and rate of loading the stress-deformation curves obtained may be linear or non-linear [101,102] which shows that the modulus is a function of the rate of loading (stress or strain range) [tensile modulus of L3-L4 = 0.88 ± 0.38 [103]. As the tensile force increased the pore in the annulus tissue matrix got diminished in sizes [104], resulting in increased diffusional drag force [105] which occurs due to the increase in the Donnan's osmotic pressure [106] (according to the Darcy's law interlaminar planes [107,108] in the annulus tissue matrix makes the

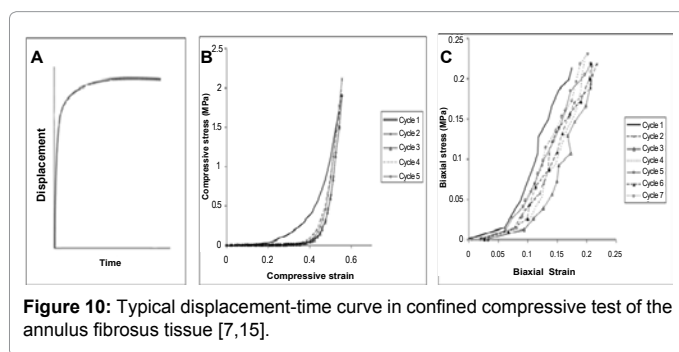


Figure 10: Typical displacement-time curve in confined compressive test of the annulus fibrosus tissue [7,15].

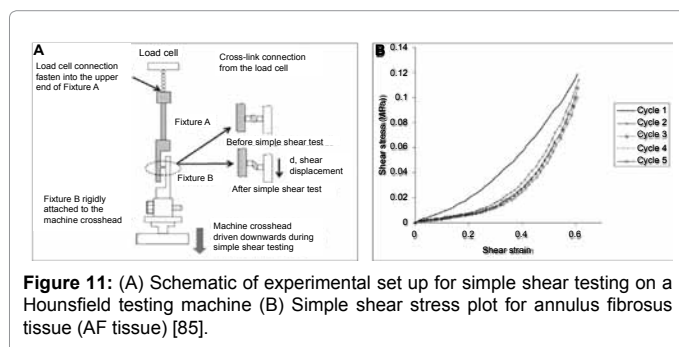


Figure 11: (A) Schematic of experimental set up for simple shear testing on a Hounsfield testing machine (B) Simple shear stress plot for annulus fibrosus tissue (AF tissue) [85].

sample very difficult to extent and finally it breaks at a yield modulus/force).

Permeability test

In addition to the confined test we can get information from the same experiment called permeability which simply indicates the resistance of fluid flow through the IVD matrix. The average fluid velocity (V_{avg}) is proportional to the pressure gradient or pressure head (Δp) which is called the Darcy's law [108] as shown in the equation (12);

$$V_{avg} = k\Delta p \quad (12)$$

The constant of proportionality is called the permeability (k), which determines the fluid (various nutrients, hormone, growth factors or gases like oxygen, carbon dioxide) flow characteristic inside the cartilage matrix [7]. The experimental set-up has been shown as (Figure 12) and the pressure head is calculated by dividing the fluid pressure difference ($p_1 - p_2$) between inside and outside of the matrix by the matrix height (h) as shown in the equation (13);

$$\Delta p = p_1 - p_2 / h \quad (13)$$

Indentation test

This test has been carried out to find out the aggregate modulus, Poisson's ratio, permeability by the fitting of the experimental data in biphasic model [109]. Indentation test is basically a confined compression test alternative for very shorter sample length about 0.8mm (Figure 13).

Tearing or fracture test

The tearing test or fracture test soft biological tissue like AF tissue is carried out by tensile testing machine. By this test we can find out the J-integral value [110] which indicates the crack propagation energy needed or fracture energy dissipated for per unit of crack extension [111]. As the soft tissue is not readily gives the crack so the tear is tested in that case by making a V- notch of say (1-3) μm at one end of the material Figure.14 (A). The other end is pulled by a tensile force by tensile tester to study the crack propagation [112] through the material which yields a similar parameter like in J-integral; similar to the tensile stress-strain failure criteria for a material. The value of J integral is calculated by the equation (14);

$$G_{p_{IC}} = Kp_{IC}^2 / E \quad (14)$$

Where $G_{p_{IC}}$ = J-integral value indicating the surface roughness, Kp_{IC} = poroelastic fracture parameter and E = elastic modulus of the material respectively [113]. Sample shape and load application for the modified single-edge notch and trouser tear tests. Each test yields a specific measure of fracture, the energy required to propagate a crack in the material [114]. The crack initiation/critical opening stress were estimated from the fracture toughness expression;

$$Kp_{IC} = \sigma_{op} \sqrt{\Pi} C_{ps} \quad (15)$$

$$\text{J-value (kN/m)} = G_{p_{IC}} = Kp_{IC}^2 / E \quad (16)$$

Kp_{IC} define where, σ_{op} is the critical opening stress of the collagen fibre where all the collagen bundle fibers start to open and becomes straight. This can be calculated from the toe-region of the stress-deformation graph. The viscoelasticity and hyperflexion [114], torsion and shear mobility of the collagen fiber makes the main contribution to initiate the strain-produced crack in the sample. The critical opening stress was calculated from the maximum load on the annulus tissue

divided by cross-sectional area of the sample [115], which is the threshold stress where collagen bundle are about to straighten along the tear force direction. The J-value or $G_{p_{IC}}$ is the main factor which determines the concentration of PG and other matrix substances inside the matrix of annulus tissue.

Lap or peeling testing

This test is done to measure the interfibrillar layers frictional force in between the AF tissue or simply interlayer frictional force by the help of nanoindentation through the help of AFM (Atomic force microscopy). This interlayer frictional value help us to gain an idea about the force required to peel off [116] the each of the AF layers from another layer i.e. matrix adhesion rigidity Figure 14 (B).

AFM (Atomic Force Microscopy) test

In this experiment with the help of nano indentation probe [117] rod the surface attribute profile or structure of the AF tissue can be studied and the matrix stiffness or roughness (roughness is calculated by Nano scope IIIA software) can be measured very accurately by this

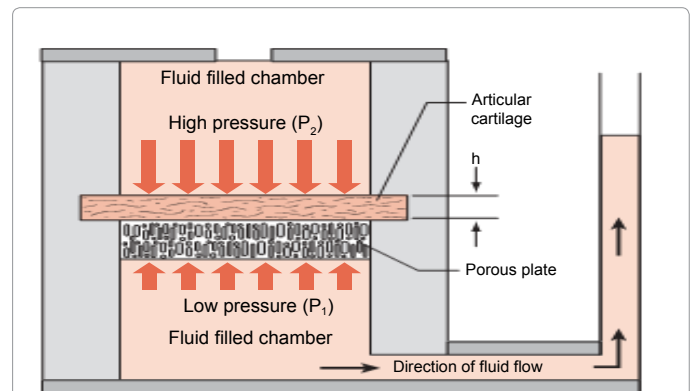


Figure 12: Schematic representation for permeability test for the annulus tissue [7].

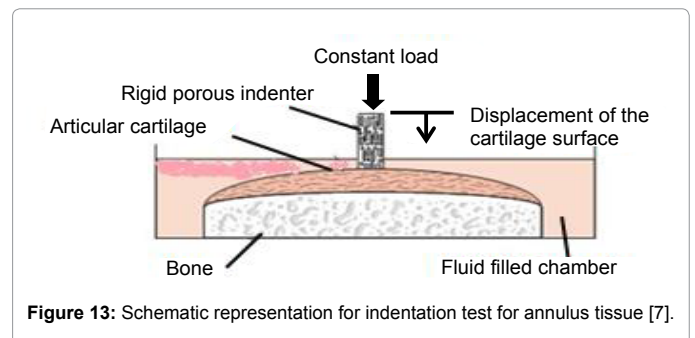


Figure 13: Schematic representation for indentation test for annulus tissue [7].

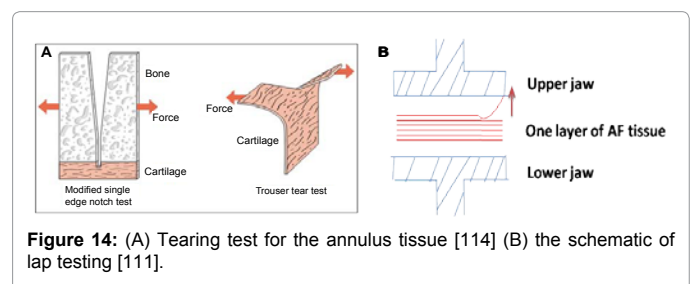


Figure 14: (A) Tearing test for the annulus tissue [114] (B) the schematic of lap testing [111].

method according to the Hertz model equation as shown by equation (17,18) which is a modified form of Young's modulus.

$$E = 3F(1 - \nu^2) / 4\sqrt{R}\delta^{3/2} \quad (18)$$

$$F = kd \quad (19)$$

Variable are; F = force, k = spring constant of the nanotip used in probing, E = elastic modulus, R = radius of curvature of the tip, ν = Poisson's ratio or indentation ratio, δ = indentation of the sample [118]. So overall we can summarize all kind of biomechanical test that can be proceed with AF tissue (Figure 15).

Confined torsion test analysis

The confined torsion modulus is much lesser than other values like compression, tensile or shear modulus due to the restricted rotational movement of the AF tissue material along its axis at a short range [118] of angle (14.5°). This angle which is called the absolute rotating angle (ARA) comes due to the particular bow-like bended structure of the human spinal axis. ARA provides the flexibility [119] and the ease of body movement by the releasing of pressure due to external loading on the spinal body [120]. The annulus fibrosus tissue also takes the rotation to this special amount of angle, ARA to maintain its continuity of attachments with the intervertebral disc body. The confined torsion modulus value of torsional modulus for bovine annulus tissue found as 0.075-0.20 MPa [80,121]. The torsion modulus is a very important factor which decides twisting forces [122] and rotating properties under small load on the disc.

The mechanical properties of AF depend not only on fiber strength, alignment and matrix composition but also on fiber-matrix interactions at the interfaces [123]. Collagen I and collagen II and proteoglycans produced by the cells play a crucial role in imbibing water, which would in turn make the AF matrix more resilient to compressive force and increase its global stiffness [80].

Reasons for disc degeneration: With the aging the disc gets dehydrated and AF tissue collapsed and put the pressure towards the surrounding nerves in the cervical area of the body and produces

lower back pain to the patient [124]. The healthy (hydrated) disc and unhealthy (dehydrated) disc has been shown (Figure 14) and degenerated disc show a distinct border between the AF and NP is still evident (arrow) [125].

The AF has retained a lamellar structure [128] however the NP is composed of mostly fibrous tissue (arrow head) (6). There may be many reasons for the disc hernia (disc radically outward bulging) which ultimately produce damage and unhealthy disc like (i) since IVD is the largest avascular tissue [129] in the human body so any change in osmotic pressure [130] in the IVD leads to its degeneration. This is happen due to the unequal force or stress distribution inside the IVD which change the porosity-dependent permeability [131] of the disc and ultimately result in loss of disc hydration and disc degeneration [130]. (ii) Production of collagen X fiber which has been delocalized in degenerated disc associated in chondrosyte clusters which lead to cleft formation and disc abnormal activities [131]. (iii) Decrease in degree of cross-linking of pyridinoline and replacing of this kind of crosslinking by the pentosidine cross-linking [125] which makes the tissue more prone to failure and increase the susceptibility of annular tear. (iv) Change in PGs synthesis: decrease of aggrecan and increase of versican, biglycan, decorin [131], KS, CS in proportional amount gives loss in hydration. So the disc will quickly degenerate. Also in this type of case the content of fibronectin will increased leads to faster disc degeneration [132,133]. (v) increase in MMPs (matrix metalloproteinases- a large family extracellular zinc based proteinases broadly divided into four subfamilies like collagenases, stromelysins, gelatinase and MT-MMPs i.e. membrane-type MMPs, examples: MMP 1,2,7,9,13) [134,135] and ADAMTS (a disintegrin and metalloprotease with thrombospondin motifs) [136,137] (6). (vi) During the life cycle the disc produced a huge amount of different MMPs in in extracellular matrix but these MMPs [138] degrade the many main cell components with it at the time of its own degeration. MMP 7,13 are more prone to disc damage by decreasing the aggrecan, collagen II particularly in NP regions (36). (vii) production of TIMPs [139,140] (tissue inhibitors of metalloproteinases, irreversible non-covalent complexes to active MMPs in a 1:1 stoichiometric fashion [139], TIMP-1 and -2) are increased the rate of disc degeneration by triggering the activity of MMPs (MMP 7) by its proteolytic action [141-146].

Alternative Idea to Replace the Disc by Some Substitute Materials: Implication of the Idea of Tissue Engineering (TE)

Low back pain affects nearly 80% the population at least once in their lifetime [147]. Degeneration of the intervertebral disc (IVD) is responsible for most cases of back pain, resulting - spinal stenosis [148], instability, disc herniation [149], radiculopathy [150] and myelopath [151]. Intervertebral disc (IVD) degeneration is thought to play an important role in producing the onset of lower back pain [51]. The center part of the disc, the nucleus pulposus (NP), which supports high compressive loads daily, shows early signs of degeneration, long before the outer part of the disc, the annulus fibrosus (AF) degenerates. So people are started to think about the physical therapy, medication or some surgical approach by the FEM (Finite Element Model) with the computational help [152] in this path TE is really a helpful substitute treatment for disc ailment. For any TE approach, we must consider four things, those are: cells, scaffolds, bioreactors and regulators [153,154]. Scaffold acts as a framework or matrix where the culture cell can grow by time and can adhere on it to regulate cell culture process. The bioreactor [155,156] acts as a server or assembly to maintain the particular condition where the scaffolds being put on with some

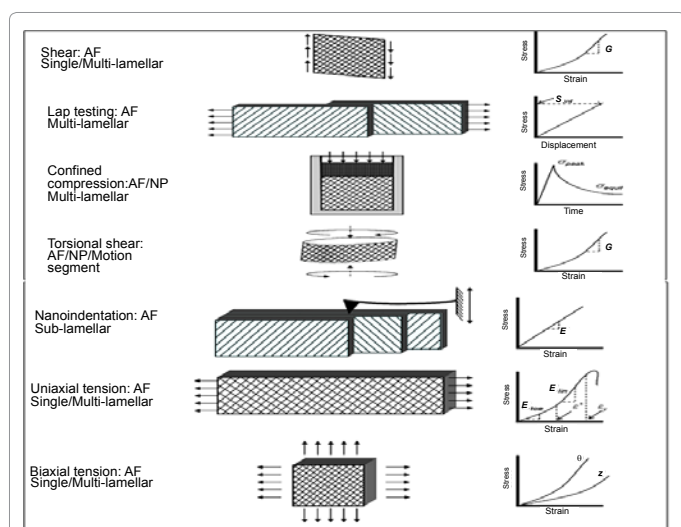


Figure 15: Schematic representations of various mechanical testing for goat AF tissue, along with typical stress-strain profiles associated with each (right). E = modulus; toe/lin = toe-region/linear region; ϵ^* = transition strain; ϵ_{yield} = yield strain; G = shear modulus; S_{int} = interfacial/lap strength; $\sigma_{speak/equilibrium}$ = peak/equilibrium stress [1].

regulator which providing a wide choices to control the different parameters for a successful tissue engineering. So a proper ECM scaffold material should be chosen for a successful TE for a body organ

Scaffold material used in tissue engineering for IVD replacement

There are many natural and synthetic materials which can be used as the matrix supporting material in the IVD/AF/NP tissue engineering as scaffolds construct, some of them are summarized (Table 2).

There may some others materials which can be used in TE for a successful IVD implantation like- atelocollagen honeycomb [159], photocrosslinked CMC (carboxymethylcellulose) for encapsulated nucleus pulposus cells [154], electrospun PVA / PVP hydrogel [160] for nucleus pulposus, the density (important for scaffold matrix stiffness characterization and workability) of the synthesized hydrogel material [161,162] is calculated by using n-heptane with the help of Denver Instruments M-120 balance by the following equation [79].

$$\rho_{\text{hydrogel}} = \rho_{\text{hydrogel}} \times m_{\text{air}} / (m_{\text{air}} - m_{\text{heptane}}) \quad (19)$$

Importance of the proper selection of scaffold structural material: obtain proper cell mechano-signal

In every cell there are certain receptors: thermoreceptors, pressure receptors or mechanoreceptors. These receptors like mechanoreceptor receive the mechanical signals and send to the brain of the body via nerve impulse, on receiving these biomechanical signals from this receptor these biosignals [163] are transformed to the necessary catastrophic [164,165] biological activities. Now how these mechanoreceptor acting as a microtransducer and able to change the biosignal to various threshold bioprocess potential to initiate the process is largely remain unknown [166]. Now using a stiffer scaffold material the mechanoreceptors of targeted organ cell could not able to get proper signal from the stem cell due to changes in protein folding as forces are exerted to expose binding sites (Figure 17) and the cells on soft matrix with weak intracellular forces cannot sufficiently alter the conformation of a mechanically-sensitive protein of interest to expose a cryptic binding site [167,168] by making it non-functional. On the other hand, cells on stiff matrix generate high tension causes the protein to unfold to a state that the binding site is hindered non-functional. However, cells on matrix with optimal elastic properties may put the appropriate amount of forces such that the cell can change the conformation of the protein, making the cryptic binding site accessible [169].

Others Methods for Disc Repair

Besides the tissue engineering there are some others techniques are also available in the market which has shown some promises for a good disc replacement as listed as (i) disc fusion - but that restricts the normalized disc movement by using of the screws. By the analysis of FEM (Finite element method) the proper IVD elemental analysis, screw optimized position, stress (Vont Mise's stress), density, volume etc [162]. The software mainly used for this purpose is ABAQUS Version 6.6 (Simulia, Providence, RI, USA) [170] by considering the kangaroo biomechanics model [152] and initial human clinical trial have indicated that an elastomeric nucleus replacement may be able to overcome these limitations. However, there is a lack of understanding of how such a device will behave in a spinal segment under large compressive loads. Furthermore, an FEA model has not been used to study the ideal characteristics of an in situ curing elastomeric device implanted from the posterolateral corner of the IVD. (ii) Gene therapy [164,166,167] - By the up and down regulation of DNA inside the gene we can repair the unhealthy disc with the help of modern gene therapy technique. (iii) Full or partial nucleotomy (85% at an angle 20° or 72% at an angle 5°) with the help of finite element meshes of the IVD models including the physiologic, nucleotomy and implant model. Nucleotomy is simply cut out the damage central part (NP) of the already degenerated disc for disc repairmen [166]. (iv) By taking some clever strategies using the concepts that chondrocytes cell moves inside the bone tissue in-vivo during the growth of the bone organ of the body [171].

Outlook of polymeric spinal implants

In the current study we try to analyze the mechanical properties of AF, NP and IVD in more details and also for the scaffolds materials that had been synthesized from the different composite materials synthesized and cell cultured for variable period from textile fibers like silk, PVA, PGA [172]. The reason to choose this textile fiber is that they are very bio-compatible and also biodegradable inside the human body. For example: the silk has been selected as scaffold material because of the following reasons: For simulating lamellae like fibrous structure of AF, the materials have to be chosen which may be used for scaffold preparation. For this project, silk fiber has been chosen to from the fibrous structure. The reason behind choosing silk as a scaffold material is that, silk offers: unique mechanical property in different material formats (about 2-3 GPa) [173] with the excellent biocompatibility, controlled degradability with the versatile process ability which thus gives a variable potential for tissue engineering applications. Moreover, the ability to process silk into different structural formats using all-

Cell source	Scaffold material	Major finding	Mechanics measured	Experimental values	Native benchmark
AF: AF cells (canine)	Alginate / chitosan hybrid fibers	AF cells proliferate and expressed collagen II, construct were nonimmunogenic upon subcutaneous implantation			
AF cells (bovine)	Electrospun PCL	AF cells oriented parallel to nanofibers and deposited aligned collagen matrix, resulting in improved tensile mechanics	Uniaxial tensile modulus	50 MPa	80-120 MPa
MSCs (bovine)	Electrospun PCL	Bi-lamellar construct replicate the +/- 30° angle-ply collagen architecture, opposing fiber arrangement enhances tensile response over parallel fiber families via inter lamellar shearing	Uniaxial tensile modulus	14.5 MPa	18 MPa
NP	Collagen I	Gel formation was tailored to replicate mechanical function, dynamic shear	Torsional shear	δ= 6.5-8.5°	23-30°
IVD: AF and NP cells (bovine)	PGA (AF) and alginate (NP)	Formed AF-NP composite ECM and increased compressive properties after implantation	Unconfined compression	Ha= 50kPa, k = 5x 10 ⁻¹⁴ m ² /(Pa s)	3-10 MPa

Table 2: Materials (Scaffolds) used in IVD tissue engineering [19,157,158,161].

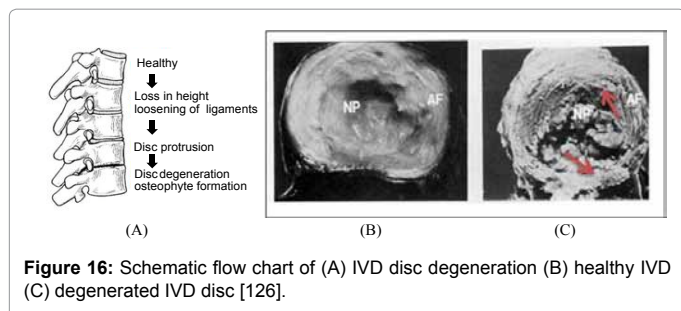


Figure 16: Schematic flow chart of (A) IVD disc degeneration (B) healthy IVD (C) degenerated IVD disc [126].

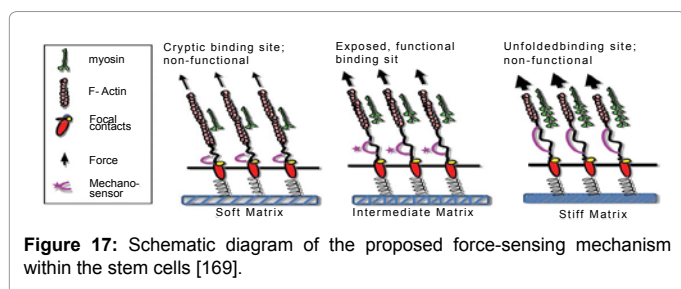


Figure 17: Schematic diagram of the proposed force-sensing mechanism within the stem cells [169].

aqueous process render it useful for the delivery of the bioactive components via this biomaterial matrix, as well as avoiding concerns for residual organic solvents in the devices. Sometime they are cross-linked with chondroitin sulfate (CS) to make it a highly bio-compatible composite tissue engineered architected structure [171]. MSC human nasal chondrosite cell is used to culture this synthesized scaffolds. Using the silk fibers, the aim would be to fabricate a structure similar to that of collagen structure of native AF. In that case, the orientation angle of fibers, diameter of fibers and fiber content in the scaffold may need to be varied [174]. So the objective of current work to simulate and experimental evaluation of the biomechanical properties of the scaffolds with the native benchmark value of IVD for a successful tissue implant which can be successfully replaced the damaged herniated disc by the tissue cultured silk scaffold disc as a better option for degenerated disc therapy.

References

- Mauck RL, Elliot DM, Nerurkar NL (2010) Mechanical design criteria for intervertebral disc tissue engineering. *J Biomech* 43: 1017-1030.
- Acaroglu ER, Iatridis JC, Setton LA, Foster RJ, Mow VC, et al. (1995) Degeneration and aging affect the tensile behavior of human lumbar annulus fibrosus. *Spine (Phila Pa 1976)* 20: 2690-2701.
- Adams MA, Roughley PJ (2006) What is intervertebral disc degeneration, and what causes it? *Spine (Phila Pa 1976)* 31: 2151-2161.
- Beckstein JC, Sen S, Schaer TP, Vresilovic EJ, Elliott DM (2008) Comparison of animal discs used in disc research to human lumbar disc: axial compression mechanics and glycosaminoglycan content. *Spine (Phila Pa 1976)* 33: E166-173.
- Bron JL, Koenderink GH, Everts V, Smit TH (2009) Rheological characterization of the nucleus pulposus and dense collagen scaffolds intended for functional replacement. *J Orthop Res* 27: 620-626.
- Little JP, Percy MJ, Tevelen G, Evans JH, Pettet G, et al. (2010) The mechanical response of the ovine lumbar annulus fibrosus to uniaxial, biaxial and shear loads. *J Mech Behav Biomed Mater* 3: 146-157.
- Mansour J (2003) *Biomechanics of Cartilage* 66-79.
- Atkinson TS, Haut RC, Altiero NJ (1998) An investigation of biphasic failure criteria for impact-induced fissuring of articular cartilage. *J Biomech Eng* 120: 536-537.
- Hayes WC, Bodine AJ (1978) Flow-independent viscoelastic properties of articular cartilage matrix. *J Biomech* 11: 407-419.
- Kempson GE (1991) Age-related changes in the tensile properties of human articular cartilage: a comparative study between the femoral head of the hip joint and the talus of the ankle joint. *Biochim Biophys Acta* 1075: 223-230.
- Johansson H, Sjolander P, Sojka P (1991) A sensory role for the cruciate ligaments. *Clin Orthop Relat Res* 268: 161-178.
- Atkinson TS, Haut RC, Altiero NJ. Impact-induced fissuring of articular cartilage: an investigation of failure criteria. *J. Biomech. Eng.* 1998; 120: 181-187.
- Oddis CV (1996) New perspectives on osteoarthritis. *Am J Med* 100: 10S-15S.
- Pickard JE, Fisher J, Ingham E, Egan J (1998) Investigation into the effects of proteins and lipids on the frictional properties of articular cartilage. *Biomaterials* 19: 1807-1812.
- Gonzalez AJ (2007) An Analysis of the Effect of Artificial Disc Replacement on The Mechanical Response of the Human Lumbar Spine. Master of Science thesis, Mechanical Engg. North Carolina State University
- van der Veen AJ, van Dieën JH, Nadort A, Stam B, Smit TH (2007) Intervertebral disc recovery after dynamic or static loading in vitro: is there a role for the endplate? *J Biomech* 40: 2230-2235
- J.P. Little, M.J. Percy, G. Jevelen, J.H. Evans, G. Pettet, C.J. Adam, *Journal of the mechanical Behaviour of Biomedical Materials*, 32, 146 (2003).
- Rohlmann A, Zander T, Schmidt H, Wilke HJ, Bergmann G (2006) Analysis of the influence of disc degeneration on the mechanical behaviour of a lumbar motion segment using the finite element method. *J Biomech* 39: 2484-2490.
- Thompson RE, Barker TM, Percy MJ (2003) Defining the neutral zone of sheep intervertebral joints during dynamic motions: An in vitro study. *Clin Biomech (Bristol, Avon)* 18: 89-98.
- Yao J, Turteltaub SR, Ducheyne P (2006) A three-dimensional nonlinear finite element analysis of the mechanical behavior of tissue engineered intervertebral discs under complex loads. *Biomaterials* 27: 377-87.
- Lehmann TR, Spratt KF, Tozzi JE, Weinstein JN, Reinartz SJ, et al. (1987) Long-term follow-up of lower lumbar fusion patients. *Spine (Phila Pa 1976)* 12: 97-104.
- Zhong ZC, Wei SH, Wang JP, Feng CK, Chen CS, et al. (2006) Finite element analysis of the lumbar Spine with a new cage using a topology optimization method. *Med Eng Phys* 28: 90-98.
- Brown T, Hansen RJ, Yorra AJ (1957) Some mechanical tests on the lumbosacral Spine with particular reference to the intervertebral discs; a preliminary report. *J Bone Joint Surg Am* 39: 1135-64.
- Shirazi-Adl A, Ahmed AM, Shrivastava SC (1986) A finite element study of a lumbar motion segment subjected to pure sagittal plane moments. *J Biomech* 19: 331-350.
- Guo LX, Teo EC (2006) Influence prediction of injury and vibration on adjacent components of Spine using finite element methods. *J Spinal Disord Tech* 19: 118-124.
- Lin HS, Liu YK, Adams KH (1978) Mechanical response of the lumbar intervertebral joint under physiological (complex) loading. *J Bone Joint Surg Am* 60: 41-55.
- Meakin JR (2001) Replacing the nucleus pulposus of the intervertebral disk: prediction of suitable properties of a replacement material using finite element analysis. *J Mater Sci Mater Med* 12: 207-13.
- Klara PM, Ray CD (2002) Artificial nucleus replacement: clinical experience. *Spine (Phila Pa 1976)* 27: 1374-1377.
- Berry JL, Moran JM, Berg WS, Steffee AD (1987) A morphometric study of human lumbar and selected thoracic vertebrae. *Spine (Phila Pa 1976)* 12: 362-367.
- Markolf KL, Morris JM (1974) The structural components of the intervertebral disc. A study of their contributions to the ability of the disc to withstand compressive forces. *J Bone Joint Surg Am* 56: 675-87.
- Virgin WJ (1951) Experimental investigations into the physical properties of the intervertebral disc. *J Bone Joint Surg Br* 33: 607-11.
- Panjabi MM, Krag M, Summers D, Videman T (1985) Biomechanical time-tolerance of fresh cadaveric human Spine specimens. *J Orthop Res* 3: 292-300.

33. Klein JA, Hukins DW (1983) Functional differentiation in the spinal column. *Eng Med* 12: 83-85.
34. Higginson GR, Litchfield MR, Snaith J (1976) Load-displacement time characteristics of articular cartilage. *Intl J Mech Sci* 18: 481-86
35. Xia Q, Wang S, Kozanek M, Passias P, Wood K, et al. (2010) In-vivo motion characteristics of lumbar vertebrae in sagittal and transverse planes. *J Biomech* 42: 705.
36. Ge Y, Maurer C, Fitzpatrick J (1996) Surface-based 3-D image registration using the iterative closest point algorithm with a closest point transform. *Med Imaging: Image process* 2710: 358-367.
37. Iatridis JC, Maclean JJ, Ryan DA (2005) Mechanical damage to the intervertebral disc annulus fibrosus subjected to tensile loading. *J Biomech* 38: 557-565.
38. Kim Y (2005) Prediction of peripheral tears in the annulus of the intervertebral disc. *Spine (Phila Pa 1976)* 25: 1771-1774.
39. O'Connell GD, Johannessen W, Vresilovic EJ, Elliott DM (2007) Human internal disc strains in axial compression measured noninvasively using magnetic resonance imaging. *Spine (Phila Pa 1976)* 32: 2860-2868.
40. Schmidt H, Kettler A, Heuer F, Simon U, Claes L, et al. (2007) Intradiscal pressure, shear strain, and fiber strain in the intervertebral disc under combined loading. *Spine (Phila Pa 1976)* 32: 748-755.
41. Adams MA (2004) Biomechanics of Back Pain. *Acupunct Med* 22:178-188.
42. Ayotte DC, Ito K, Perren SM, Tepic S (2000) Direction-dependent constriction flow in a poroelastic solid: the intervertebral disc valve. *J Biomech Eng* 122: 587-593.
43. van Dieen JH, Kingma I, Meijer R, Hansel L, Huiskes R (2001) Stress distribution changes in bovine vertebrae just below the endplate after sustained loading. *Clin Biomech (Bristol, Avon)* 16: S135-S142.
44. Wilke HJ, Neef P, Caimi M, Hoogland T, Claes LE (1999) New in vivo measurements of pressures in the intervertebral disc in daily life. *Spine (Phila Pa 1976)* 24: 755-762.
45. Tyrrell AR, Reilly T, Troup JD (1985) Circadian variation in stature and the effects of spinal loading. *Spine (Phila Pa 1976)* 10: 161-164.
46. Le Maitre CL, Hoyland JA, Freemont AJ (2007) Catabolic cytokine expression in degenerate and herniated human intervertebral discs: IL-1beta and TNFalpha expression profile. *Arthritis Res Ther* 9:R77.
47. Farndale RW, Buttle DJ, Barrett AJ (1986) Improved quantitation and discrimination of sulphated glycosaminoglycans by use of dimethylmethylene blue. *Biochim Biophys Acta* 883: 173-177.
48. Holm S, Maroudas A, Urban JP, Selstam G, Nachemson A (1981) Nutrition of the intervertebral disc: solute transport and metabolism. *Connect Tissue Res* 8: 101-119.
49. Wallach CJ, Sobajima S, Watanabe Y, Kim JS, Georgescu HI, et al. (2003) Gene transfer of the catabolic inhibitor TIMP-1 increases measured proteoglycans in cells from degenerated human intervertebral discs. *Spine (Phila Pa 1976)* 28: 2331-2337.
50. Luoma K, Riihimäki H, Luukkonen R, Raininko R, Viikari-Juntura E, et al. (2000) Low back pain in relation to lumbar disc degeneration. *Spine (Phila Pa 1976)* 25: 487-492.
51. Le Maitre CL, Pockert A, Buttle DJ, Freemont AJ, Hoyland JA (2007) Matrix synthesis and degradation in human intervertebral disc degeneration. *Biochem Soc Trans* 35: 652-655.
52. Risbud MV, Izzo MW, Adams CS, Arnold WW, Hillibrand AS, et al. (2003) An organ culture system for the study of the nucleus pulposus: description of the system and evaluation of the cells. *Spine (Phila Pa 1976)* 28: 2652-2658.
53. MacLean JJ, Lee CR, Alini M, Iatridis JC (2005) The effects of short-term load duration on anabolic and catabolic gene expression in the rat tail intervertebral disc. *J Orthop Res* 23: 1120-1127.
54. Richardson SM, Mobasher A, Freemont A J, Hoyland JA (2007) Intervertebral disc biology, degeneration and novel tissue engineering and regenerative medicine therapies. *Histol Histopathol* 22: 1033-1041.
55. Korecki CL, Maclean JJ, Iatridis JC (2007) Characterization of an in vitro intervertebral disc organ culture system. *Eur Spine J* 16: 1029-1037.
56. Tamini MI, Day, AJ, Turley EA (2002) Hyaluronan and homeostasis: a balancing act. *J Biol Chem* 277: 4581-4584.
57. Girish KS, Kemparaju K (2007) The magic glue hyaluronan and its eraser hyaluronidase: A biological overview. *Life Sci* 80: 1921-1943.
58. Jurvelin JS, Buschmann MD, Hunziker EB (1997) Optical and mechanical determination of poisson's ratio of adult bovine humeral articular cartilage. *J Biomech* 30: 235-241.
59. Armstrong CG, Lai WM, Mow VC (1984) An analysis of the unconfined compression of articular cartilage. *J Biomech Eng* 106: 165-173.
60. Buschmann MD, Jurvelin JS, Hunziker EB (1995) Comparison of sinusoidal and stress relaxation measurements of cartilage in confined compression: The biphasic poroelastic model and the role of the porous compressing platen. *Trans Orthop Rex Soc* 20: 521.
61. Hayes WC, Keer LM, Herrman G, Mockros LF (1972) A mathematical analysis for indentation tests of articular cartilage. *J Biomech* 5: 541-551.
62. Spilker RL, Suh JK, Mow VC (1990) Effects of friction on the unconfined compressive response of articular cartilage: a finite element analysis. *J Biomech Eng* 112: 138- 146.
63. Mak AF, Lai WM, Mow VC (1987) Biphasic indentation of articular cartilage--I. Theoretical analysis. *J Biomech* 20: 703-714.
64. K. Singha, Master of Technology thesis, Biomechanical characterization of silk fibre-ECM composite Intervertebral Disc (IVD) tissue constructs, Textile Tech. Indian Institute of Technology, Delhi, 2011.
65. Magnier C, Boiron O, Wendling-Mansuy S, Chabrand P, Deplano V (2009) Nutrient distribution and metabolism in the intervertebral disc in the unloaded state: a parametric study. *J Biomech* 42: 100-108.
66. Jacobs NT, Morelli J, Smith LJ et al., "Annulus fibrosus shear mechanical properties and the contributions of glycosaminoglycans and elastic fibers shear are anisotropic" (Transactions of the 56th Annual Meeting of the Orthopaedic Research Society, New Orleans, LA., 2010).
67. Adams MA, Freeman BJ, Morrison HP, Nelson IW, Dolan P (2000) Mechanical initiation of intervertebral disc degeneration. *Spine (Phila Pa 1976)* 25: 1625-1636.
68. Kerttula LI, Serlo WS, Tervonen OA, Paakko EL, Vanharanta HV (2000) Post-traumatic findings of the Spine after earlier vertebral fracture in young patients: clinical and MRI study. *Spine (Phila Pa 1976)* 25: 1104-1108.
69. Pollintine P, Przybyla AS, Dolan P, Adams MA (2004) Neural arch load-bearing in old and degenerated Spines. *J Biomech* 37: 197-204.
70. Adams MA, Dolan P (2005) Spine biomechanics. *J Biomech* 38: 1972-1983.
71. Perowicz CA, Robertson PA, Broom ND (2005) Intralamellar relationships within the collagenous architecture of the annulus fibrosus imaged in its fully hydrated state. *J Anat* 207: 299-312.
72. JP Little, G Tevelen, CJ Adam, JH Evans, MJ Pearcy (2009) Development of a biaxial compression device for biological samples: Preliminary experimental results for a closed cell foam. *J Mech Behav Biomed Mater* 2: 305-309.
73. Michalek AJ, Buckley MR, Bonassar LJ, Cohen I, Iatridis JC (2009) Measurement of local strains in intervertebral disc annulus fibrosus tissue under dynamic shear: contributions of matrix fiber orientation and elastin content. *J Biomech* 42: 2279-2285.
74. Pezowicz CA, Robertson PA, Broom ND (2006) The structural basis of interlamellar cohesion in the intervertebral disc wall. *J Anat* 208: 317-330.
75. Marchand F, Ahmed AM (1990) Investigation of the laminate structure of lumbar disc annulus fibrosus. *Spine (Phila Pa 1976)* 15: 402-410.
76. Guerin HL, Elliot DM (2007) Quantifying the contributions of structure to annulus fibrosus mechanical function using a nonlinear, anisotropic, hyperelastic model. *J Orthop Res* 25: 508-516
77. Viidik A (1973) Functional properties of collagenous tissues. *Int Rev Connect Tissue Res* 6: 127-215.
78. Bland JM, Altman DG (1986) Statistical methods for assessing agreement between two methods of clinical measurement. *Lancet* 1: 307-310.
79. Iatridis JC, ap Gwynn I (2004) Mechanisms for mechanical damage in the intervertebral disc annulus fibrosus. *J Biomech* 37: 1165-1175.

80. Seroussi RE, Krag MH, Muller DL, Pope MH (1989) Internal deformations of intact and denucleated human lumbar discs subjected to compression, flexion, and extension loads. *J Orthop Res* 7: 122-131.
81. Natarajan RN, Ke JH, Andersson GB (1984) A model to study the disc degeneration process. *Spine (Phila Pa 1976)* 19: 259-265.
82. Lynch HA, Johannessen W, Wu JP, Jawa A, Elliott DM (2003) Effect of fiber orientation and strain rate on the nonlinear uniaxial tensile material properties of tendon. *J Biomech Eng* 125: 726-731.
83. Guerin HA, Elliott DM (2006) Degeneration affects the fiber reorientation of human annulus fibrosus under tensile load. *J Biomech* 39: 1410-1418.
84. Simon BR, Wu JS, Carlton MW, Evans JH, Kazarian LE (1985) Structural Models for Human Spinal Motion Segments Based on a Poroelastic View of the Intervertebral Disk. *J Biomech Eng* 107: 327-335.
85. Wagner DR, Lotz JC (2004) Theoretical model and experimental results for the nonlinear elastic behavior of human annulus fibrosus. *J Orthop Res* 22: 901-909.
86. Aspden RM (2005) Agreement between two experimental measures or between experiment and theory. *J Biomech* 38: 2136-2137.
87. Hansen KA, Weiss JA, Barton JK (2002) Recruitment of tendon crimp with applied tensile strain. *J Biomech Eng* 124: 72-77.
88. Klisch SM, Lotz JC (1999) Application of a fiber-reinforced continuum theory to multiple deformations of the annulus fibrosus. *J Biomech* 32: 1027-1036.
89. Banse X, Devogelaer JP, Munting E, Delloye C, Cornu O, et al. (2001) Inhomogeneity of human vertebral cancellous bone: systematic density and structure patterns inside the vertebral body. *Bone* 28: 563-71
90. Kulak RF, Belytschko TB, Schultz AB (1976) Nonlinear behavior of the human intervertebral disc under axial load. *J Biomech* 9: 377-386.
91. Panagiotopoulos ND, Knauss, WG, Bloch R (1979) On the mechanical properties of human intervertebral disc material. *Biorheology* 16: 317-330.
92. Gruber HE, Hanley Jr EN (2002) Ultrastructure of the human intervertebral disc during aging and degeneration: comparison of surgical and control specimens. *Spine (Phila Pa 1976)* 27: 798-805.
93. Meakin JR, Hukins DW (2000) Effect of removing the nucleus pulposus on the deformation of the annulus fibrosus during compression of the intervertebral disc. *J Biomech* 33: 575-580.
94. Adams MA, McNally DS, Dolan P (1996) 'Stress' distributions inside intervertebral discs. The effects of age and degeneration. *J Bone Joint Surg Br* 78: 965-975.
95. Adams MA, Hutton WC (1983) The effect of posture on the fluid content of lumbar intervertebral discs. *Spine (Phila Pa 1976)* 8: 665-671.
96. Osti OL, Vernon-Roberts B, Fraser RD (1990) Annulus tears and intervertebral disc degeneration: an experimental study using an animal model. *Spine* 15: 762-767.
97. Dunlop RB, Adams MA, Hutton WC (1984) Disc space narrowing and the lumbar facet joints. *J Bone Joint Surg Br* 66: 706-810.
98. Moneta GB, Videman T, Kaivanto K, Aprill C, Spivey M, et al. (1994) Reported pain during lumbar discography as a function of annular ruptures and disc degeneration: a re-analysis of 833 discograms. *Spine* 19: 1968-1974.
99. Quinell RC, Stockdale HR, Willis DS (1983) Observations of pressures within normal discs in the lumbar spine. *Spine* 8: 166-169.
100. Schwarzer AC, Aprill CN, Derby R, Fortin J, Kine G, et al. (1995) The prevalence and clinical features of internal disc disruption in patients with chronic low back pain. *Spine* 20: 1878-1883.
101. Tanaka M, Nakahara S, Inoue H (1993) A pathologic study of discs in the elderly: separation between the cartilaginous endplate and the vertebral body. *Spine* 18: 1456-1462.
102. Vernon-Roberts B (1988) Disc pathology and disease states. Ghosh P, ed. *The biology of the intervertebral disc. Volume II.* Boca Raton, Florida: CRC Press Inc. 73-119.
103. Maroudas A (1968) Physicochemical properties of cartilage in the light of ion exchange theory. *Biophys J* 8: 575-595.
104. Hayes WC, Mockros LF (1971) Viscoelastic properties of human articular cartilage. *J Appl Physiol* 31:562-568.
105. Stok K, Oloyede A. (2007) Conceptual fracture parameters for articular cartilage. *Clin Biomech* 22: 725-735.
106. Finlay JB, Repo RU (1978) Instrumentation and procedure for the controlled impact of articular cartilage. *IEEE Trans Biomed Eng* 25: 34-39.
107. Meachim G, Sheffield SR (1969) Surface ultrastructure of mature adult human articular cartilage. *J Bone Joint Surg Br* 51B: 529-539.
108. Purslow PP (1983) Measurement of the fracture toughness of extensible connective tissues. *J Mat Sci* 18: 3591-3598.
109. Radin EL, Paul IL, Lowy M (1970) A comparison of the dynamic force transmitting properties of subchondral bone and articular cartilage. *J Bone Joint Surg Am* 52: 444-456.
110. Rivlin RS, Thomas AG (1953) Rupture of rubber. I. characteristic energy for tearing. *J Polymer Sci* 10: 291-318.
111. Stok K, Oloyede A (2003) A qualitative analysis of crack propagation in articular cartilage at varying rates of tensile loading. *Connect Tissue Res* 44: 109-120.
112. Lewis NT, Hussain MA, Mao JJ (2008) Investigation of nano-mechanical properties of annulus fibrosus using atomic force microscopy. *Micron* 39: 1008-1019.
113. Wu HW, Kuhn T, Moy VT (1998) Mechanical properties of L929 cells measured by atomic force microscopy: effects of anticytoskeletal drugs and membrane crosslinking. *Scanning* 20: 389-397.
114. Amarantini D, Rao G, Berton E (2010) A two-step EMG-and-optimization process to estimate muscle force during dynamic movement. *J Biomech* 43:1827-1830.
115. Bobbert MF, van Ingen-Schenau GJ (1988) Coordination in vertical jumping. *J Biomech* 21: 249-262.
116. Thelen DG, Anderson FC, Delp SL (2003) Generating dynamic simulations of movement using computed muscle control. *J Biomech* 36: 321-328.
117. Zajac FE (1989) Muscle and tendon: properties, models, scaling, and application to biomechanics and motor control. *Crit Rev Biomed Eng* 17: 359-411.
118. Crowninshield RD, Brand RA (1981) A physiologically based criterion of muscle force prediction in locomotion. *J Biomech* 14: 793-801.
119. Cui M, Wan Y, Anderson DG, Shen FH, Leo BM, et al. (2008) Mouse growth and differentiation factor-5 protein and DNA therapy potentiates intervertebral disc cell aggregation and chondrogenic gene expression. *Spine J* 8: 287-295.
120. Handa T, Ishihara H, Ohshima H, Osada R, Tsuji H, et al. (1997) Effects of hydrostatic pressure on matrix synthesis and matrix metalloproteinase production in the human lumbar intervertebral disc. *Spine* 22: 1085-1091.
121. Kanemoto M, Hukuda S, Komiya Y, Katsuura A, Nishioka J (1996) Immunohistochemical study of matrix metalloproteinase-3 and tissue inhibitor of metalloproteinase-1 human intervertebral discs. *Spine* 21: 1-8.
122. Wehling P, Schultiz KP, Robbins PD, Evans CH, Reinecke JA (1997) Transfer of genes to chondrocytic cells of the lumbar spine. Proposal for a treatment strategy of spinal disorders by local gene therapy. *Spine* 22: 1092-1097.
123. Antoniou J, Steffen T, Nelson F, Winterbottom N, Hollander AP, et al. (1996) The human lumbar intervertebral disc: evidence for changes in the biosynthesis and denaturation of the extracellular matrix with growth, maturation, ageing, and degeneration. *J Clin Invest* 98: 996-1003.
124. Moon SH, Gilbertson LG, Nishida K, Knaub M, Muzzonigro T, et al. (2000) Human intervertebral disc cells are genetically modifiable by adenovirus-mediated gene transfer: implications for the clinical management of intervertebral disc disorders. *Spine* 25: 2573-2579.
125. Nishida K, Kang JD, Suh JK, Robbins PD, Evans CH, et al. (1998) Adenovirus-mediated gene transfer to nucleus pulposus cells. Implications for the treatment of intervertebral disc degeneration. *Spine* 23: 2437-2442.
126. Thompson JP, Oegema TR Jr, Bradford DS (1991) Stimulation of mature canine intervertebral disc by growth factors. *Spine* 16: 253-260.
127. Fujita Y, Wagner DR, Biviji AA, Duncan NA, Lotz JC (2000) Anisotropic shear behavior of the annulus fibrosus: effect of harvest site and tissue prestrain. *Med Eng Phys* 22:349-357.
128. Joshi A, Fussell G, Thomas J, Hsuan A, Lowman A (2006) Functional

- compressive mechanics of a PVA/PVP nucleus pulposus replacement. *Biomaterials* 27:176-184.
129. Baumgartner W (1994) Intervertebral disk prosthesis. US Patent No.5320644.
130. Salib RM, Pettine KA (1993) Intervertebral disk arthroplasty. US Patent No. 5258031.
131. Iatridis JC, Weidenbaum M, Setton LA, Mow VC (1996) Is the nucleus pulposus a solid or a fluid? Mechanical behaviors of the nucleus pulposus of the human intervertebral disc. *Spine* 21: 1174-1184.
132. Lee CK, Langrana NA (1984) Lumbosacral spinal fusion: a biomechanical study. *Spine* 9: 574-581.
133. Patil A (1982) Artificial intervertebral disc. US Patent No. 4309777.
134. Huttmacher DW, Ng KW, Kaps C, Sittinger M, Klaring S (2003) Elastic cartilage engineering using novel scaffold architectures in combination with a biomimetic cell carrier. *Biomaterials* 24: 4445-4458.
135. Stammen JA, William S, Ku DN, Guldberg RE (2001) Mechanical properties of a novel PVA/PVP hydrogel in shear and unconfined compression. *Biomaterials* 22: 799-806.
136. Thomas J, Gomes K, Lowman A, Marcolongo M (2004) The effect of dehydration history on PVA/PVP hydrogels for nucleus pulposus replacement. *J Biomed Mater Res B Appl Biomater* 69: 135-140.
137. Bao QB, Higham PA (1991) Hydrogel intervertebral disc nucleus. US Patent No. 5047055.
138. Shirazi-Adl SA, Shrivastava SC, Ahmed AM (1984) Stress analysis of the lumbar disc-body unit in compression. A three-dimensional nonlinear finite element study. *Spine* 9: 120-134.
139. Bao QB, Higham PA (1993) Hydrogel intervertebral disc nucleus. US Patent No. 5192326.
140. Tiberwal SB, Pearcy MJ, Portek I, Spivey J (1985) A prospective study of lumbar spinal movements before and after discectomy using biplanar radiography. Correlation of clinical and radiographic findings. *Spine* 10: 455-460.
141. Fussell G, Thomas J, Scanlon J, Lowman A, Marcolongo M (2005) The effect of protein-free versus protein-containing medium on the mechanical properties and uptake of ions of PVA/PVP hydrogels. *J Biomater Sci Polym Ed* 16: 489-503.
142. Inkinen RI, Lammi MJ, Agren U, Tammi R, Puustjärvi K, et al. (1999) Hyaluronan Distribution in the Human and Canine Intervertebral Disc and Cartilage Endplate. *Histochem J* 31: 579-587.
143. Aguiar DJ, Johnson SL, Oegema TR (1999) Notochordal Cells Interact with Nucleus Pulposus Cells: Regulation of Proteoglycan Synthesis. *Exp Cell Res* 246: 129-137.
144. Cleaver CS, Rowan AD, Cawston TE (2001) Interleukin 13 blocks the release of collagen from bovine nasal cartilage treated with proinflammatory cytokines. *Ann Rheum Dis* 60:150-157.
145. T.R. Sabet, J. Choi, A. Diwan, paper presented at the 7th annual Scientific Meeting of the Spine Arthroplasty Society, Berlin, Germany, May 2007.
146. Strange DG, Fisher ST, Boughton PC, Kishen TJ, Diwan AD (2010) Restoration of compressive loading properties of lumbar discs with a nucleus implant-a finite element analysis study. *Spine J* 10: 602-609.
147. Thompson JP, Pearce RH, Schechter MT, Adams ME, Tsang IK (1990) Preliminary evaluation of a scheme for grading the gross morphology of the human intervertebral disc. *Spine* 15: 411-415.
148. Reza AT, Nicoll SB (2010) Characterization of novel photocrosslinked carboxymethylcellulose hydrogels for encapsulation of nucleus pulposus cells. *Acta Biomater* 6: 179-186.
149. Gruber HE, Fisher EC Jr, Desai B, Stasky AA, Hoelscher G, et al. (1997) Human intervertebral disc cells from the annulus: three-dimensional culture in agarose or alginate and responsiveness to TGF-beta1. *Exp Cell Res* 235: 13-21.
150. Bryant SJ, Durand KL, Anseth KS (2003) Manipulations in hydrogel chemistry control photoencapsulated chondrocyte behavior and their extracellular matrix production. *J Biomed Mater Res A* 67: 1430-1436.
151. Burdick JA, Chung C, Jia X, Randolph MA, Langer R (2005) Controlled degradation and mechanical behavior of photopolymerized hyaluronic acid networks. *Biomacromolecules* 6: 386-391.
152. Chung C, Mesa J, Miller GJ, Randolph MA, Gill TJ, et al. (2006) Effects of auricular chondrocyte expansion on neocartilage formation in photocrosslinked hyaluronic acid networks. *Tissue Eng* 12: 2665-2673.
153. Iwasa J, Ochi M, Uchio Y, Katsube K, Adachi N, et al. (2003) Effects of cell density on proliferation and matrix synthesis of chondrocytes embedded in atelocollagen gel. *Artif Organs* 27: 249-255.
154. Roughley P, Hoemann C, DesRosiers E, Mwale F, Antoniou J, et al. (2006) The potential of chitosan-based gels containing intervertebral disc cells for nucleus pulposus supplementation. *Biomaterials* 27: 388-396.
155. Nguyen KT, West JL (2002) Photopolymerizable hydrogels for tissue engineering applications. *Biomaterials* 23: 4307-4314.
156. Tover A, Gano SE, Mason JJ, Renuad JE (2005) Optimum design of an interbody implant for lumbar spine fixation. *Adv Eng Softw* 36: 634-642.
157. Davis H (1994) Increasing rates of cervical and lumbar spinal surgery in the United States, 1979-1990. *Spine* 19: 1117-1124.
158. Bendsøe MP (1989) Optimal shape design as a material distribution problem. *Struct Optim* 1: 193-200.
159. Tovar A, Renaud JE, Mason JJ (2003) Optimum topology design of an interbody fusion implant for lumbar spine fixation. In: Eighth international conference on computer aided optimum design of structures.
160. Zander T, Rohlmann A, Klockner C, Bergmann G (2002) Comparison of the mechanical behavior of the lumbar spine following mono- and bisegmental stabilization. *Clin Biomech* 17: 439-445.
161. Fung YC (1993) *Biomechanics. Mechanical properties of living tissues*. New York: Springer-Verlag.
162. Rohlmann A, Neller S, Claes L, Bergmann G, Wilke HJ (2001) Influence of a follower load on intradiscal pressure and intersegmental rotation of the lumbar spine. *Spine* 26: E557-E561.
163. Sigmund O (2001) A 99 line topology optimization code written in matlab. *Struct Multidisc Optim* 21: 120-127.
164. Livecoff EA, Gilbertson MD, Kang JD (2005) Gene therapy for disc repair. *Spine J* 5: 287S-296S.
165. Morales TI (2007) Chondrocyte moves: clever strategies? *Osteoarthritis and Cartilage* 15: 861-871.
166. Schneller M, Vouri K, Rouslathi E (1997) Alphavbeta3 integrin associates with activated insulin and PDGFbeta receptors and potentiates the biological activity of PDGF. *EMBO J* 16: 5600-5607.
167. Wang W, Wyckoff JB, Frohlich VC, Oleynikov Y, Hüttelmaier S, et al. (2002) Single cell behavior in metastatic primary mammary tumors correlated with gene expression patterns revealed by molecular profiling. *Cancer Res* 62: 6278-6288.
168. Bush PG, Hall AC (2003) The volume and morphology of chondrocytes within non-degenerate and degenerate human articular cartilage. *Osteoarthritis Cartilage* 11: 242-251.
169. Fujita T, Azume Y, Fukuyama R, Hattori Y, Yoshida C, et al. (2004) Runx2 induces osteoblast and chondrocyte differentiation and enhances their migration by coupling with PI3K-Akt signaling. *J Cell Biol* 166: 85-95.
170. Roberts S, Evans H, Trivedi J, Menage J (2006) Histology and pathology of the human intervertebral disc. *J Bone Joint Surg* 88: 10-14.
171. Wang Q, Breinan HA, Hsu HP, Spector M (2000) Healing of defects in canine articular cartilage: distribution of non-vascular alpha-smooth muscle actin-containing cells. *Wound Repair Regen* 8: 145-158.
172. Kim KW, Lim TH, Kim JG, Jeong ST, Masuda K (2003) The origin of chondrocytes in the nucleus pulposus and histologic findings associated with the transition of a notochordal nucleus pulposus in intact rabbit intervertebral discs. *Spine* 28: 982-990.
173. Sinsawat A, Putthanavat S, Magoshi Y, Pachter R, Eby RK (2003) The crystal modulus of silk (*Bombyx mori*). *Polymer* 44: 909-910.
174. Kaplan D, Adams WW, Farmer BL, Viney C (1994) Silk polymers: materials science and biotechnology. American Chemical Society, ACS symposium series 544.